Proceedings of ASME Turbo Expo 2011
GT2011
June 6-10, 2011, Vancouver, British Columbia, Canada

GT2011-45262

MEASUREMENT OF A BENCHMARKING JET IN CROSSFLOW CONFIGURATION UNDER HIGHLY TURBULENT CONDITIONS

Camilo Cárdenas*
Julia Sedlmaier
Nikolaos Zarzalis

Division for Combustion Technology
Karlsruhe Institute of Technology
Karlsruhe, Germany

Richard J. Valdes

Siemens Energy, Inc. EN 323

Werner Krebs

Siemens AG PG PE3

ABSTRACT

The configuration of a jet in crossflow appears in many practical applications such as combustion and mixing processes in the chemical industry. This kind of flow is particularly complex due to the presence of various interacting vortex systems and it is widely studied in literature both experimentally and numerically. In addition to the physical interest, this flow configuration serves as a benchmark for numerical methods such as Direct Numerical Simulations (DNS) and Large Eddy Simulations (LES) because of its prototypic nature.

The present work aims at generating benchmark data for a jet in crossflow configuration under highly turbulent conditions. In this context, the investigated operating conditions were chosen carefully to match the conditions existing in gas turbines and hence the experiments were carried out for two different Reynolds-numbers of the crossflow, Re_∞ = 60000 and 40000. Keeping the flow rate of the jet flow constant, two different velocity ratios between jet and crossflow of r = 4.15 and 6.25 result. The measurements were performed in an appropriate air channel, which was built with the objective to obtain accurately controlled flow conditions at the measurement section. Two-dimensional laser induced fluorescence (2d-LIF) combined with particle imaging velocimetry (PIV) was used for the measurements of simultaneous scalar concentration and velocity fields and the experimental acquisition of Reynolds-fluxes and -stresses. The knowledge of Reynolds-fluxes and -stresses is of fundamental concern not only for the understanding of the mechanisms which are responsible for the formation of the vortex-structures in a jet in crossflow, but also for the development and validation of turbulence- and mixing-models.

NOMENCLATURE

$< u >$, $< v >$, $< w >$	Time averaged velocity in x, y, z-direction, respectively [m/s].
$DEHS$	Di-Ethyl-Hexyl-Sebacat.
D	Jet diameter, 8 mm.
D_∞	Hydraulic diameter of the crossflow, 108 mm.
U	Bulk velocity, [m/s].
LIF	Laser induced fluorescence.
JCF	Jet in crossflow.
PIV	Particle image velocimetry.
LES	Large-Eddy simulation.
DNS	Direct numerical simulation.
RANS	Reynolds-averaged Navier-Stokes.

*camilo.cardenas@kit.edu

Tu	Turbulence intensity, [%].
$< c >$	Time averaged, normalized jet concentration.
$< C_{NO_2} >$	Time averaged NO_2-concentration, [ppm].
$C_{NO_2,j}$	Initial NO_2-concentration in jet-flow, [ppm].
$_\infty$	Crossflow parameter.
$_j$	Jet parameter.
$_\sigma$	Standard deviation.
$'$	Temporal fluctuation.
r	Velocity ratio, dimensionless.
Re	Reynolds-number, dimensionless.
Nl	Norm-liter, Liter at 1 atm and 273 K.

INTRODUCTION

The jet in crossflow (JCF) arrangement is a simple flow disposition, in which a jet is injected perpendicular into a crossflow. This kind of arrangement appears in many technical devices like gas turbines and mixers in the process industry. The potential of a JCF to mix fluid streams allows not only more efficient but also a faster mixing processes than other flow configurations as for example straight jets [1–3]. The latter is taken into consideration for example by gas turbine manufacturers to be applied to the lean premix burner technology, where the fuel and combustion air streams are premixed before reaching the combustion chamber. In this regard, a JCF appears as a suitable flow disposition for this aim, where the jet-flow must rapidly penetrate the crossflow in order to accomplish the mixing in a short distance. Consequently, the flow conditions commonly used in such technical applications are highly turbulent and therefore the application of Direct Numerical Simulations (DNS) to design and/or predict the flow pattern is unprofitable and limited. In this connection, Large-Eddy-Simulations (LES) and Reynolds-Averaged Navier-Stokes (RANS) simulations are employed as an alternative to this purpose. In these approaches Reynolds-fluxes $< v_i'c' >$ and stresses $< v_i'v_k' >$ appear as additional terms leading to a closure problem of the corresponding mean conservation equations. Therefore, these terms have to be modeled. In order to develop and validate appropriate models, ample experimental data especially for the Reynolds-fluxes and stresses has to be available. These quantities reflect the enhanced fluxes of a turbulent flow compared to a laminar one, thus they are of particular interest.

In contrast to most of the works known in the literature, which are dedicated to the investigation mechanisms responsible for the formation of the vortex-structures of the JCF [4], an experimental investigation of two JCF-configurations under highly turbulent conditions by means of simultaneous 2d-LIF and PIV measurements was undertaken. Some simultaneous PIV- and 2d-LIF-measurements under reactive and non-reactive conditions are known from the literature [5–11], nevertheless only few deal with the JCF-configuration [7, 9–11] and they are carried out, in contrast with the present investigation, under flow conditions which are far from being considered as highly turbulent. Recently, Galeazzo et al. [12] presented a combined numerical and experimental work concerning on the investigation of the turbulent mixing within the jet in crossflow under highly turbulent conditions. The current study intends to continue this approach, aiming at the creation of an experimental data base for different highly turbulent JCF-configurations. For this purpose, 2d-LIF-PIV measurement of the same flow conditions of Galeazzo et al. [12, 13] and of a new study case with a new boundary condition have been carried out. The present paper differs from previous works in that: (1) the experimental inflow-conditions of both flows have been carefully determined and reported, (2) experimental 2d-maps of Reynolds-fluxes and -stresses for the symmetry plane of a JCF-configuration under highly turbulent conditions have been reported.

EXPERIMENTAL SETUP

Flow Configuration and measurement technique

The experiments were performed in an open circuit, horizontal air channel, which is described in detail in Cárdenas et al. [9, 11]. Taking into consideration some performed modifications at the arrangement, a short overview is given in this section. Figure 1 shows a schematic illustration of the flow channel and the feed pipes of both, the crossflow and the jet-flow. In most cases, the flow conditions in a JCF-arrangement are characterized by the Reynolds-number of the crossflow $Re_\infty = U_\infty \cdot D_\infty / \nu$ and the momentum-flux ratio $R = \rho_j U_j^2 / \rho_\infty U_\infty^2$ between jet and crossflow, which for equal-density flows $\rho_j = \rho_\infty$ can be simplified to the velocity ratio $r = U_j / U_\infty$. With U_∞ as the crossflow bulk velocity, D_∞ = 108 mm as characteristic length or rather the hydraulic diameter of the crossflow, and ν as the kinematic viscosity. The subscript index j identifies the parameters of the jet-flow and the subscript index ∞ the ones of the crossflow. The setup allowed a very wide range of Reynolds-numbers for the crossflow $700 \leq Re_\infty \leq 360 \times 10^3$ as well as for the jet $150 \leq Re_j \leq 26.5 \times 10^3$.

A fan was used to blow air from the environment into the feed pipe system of the crossflow and with a combination of three parallel venturi tubes the flow rate of the air was adjusted. Additionally, Di-Ethyl-Hexyl-Sebacat (DEHS) liquid droplets, necessary for the PIV-measurements, were added to the crossflow at the diffusor's entrance (cf. Fig. 1) and to the jet flow by two separate aerosol generators. The aerosol generators were fed by the compressed air network of the building. For this purpose two mass flow controllers were employed with maximal flow rates of about 40 Nl/min air and 10 Nl/min air respectively.

The jet pipe has an inner diameter D = 8 mm, and the measuring section a square sectional area of 108 mm × 108 mm. To set up the jet flow-conditions to be investigated, an air stream from the compressed air network of the building, a gas cylinder of 100% NO_2 and the already mentioned air flow loaded with aerosol droplets for the jet were combined. The air stream was controlled using a mass flow meter with a maximal flow rate of 250 *Nl*/min air and the corresponding NO_2 mass flow was regulated by a needle valve obtaining a constant concentration of NO_2 in the jet-flow of 1.5% (vol). NO_2 was used as molecular tracer for the LIF measurements – see below. Since NO_2 is characterized by a small vapor pressure, the NO_2 gas cylinder was heated by an electric blanket to avoid possible condensation of NO_2 in the feed-line and consequently to warrant a good mixing of the tracer with the air of the jet-flow. Generally, the temperature of the crossflow was higher than the one of the unregulated jet (up to 25 K); therefore the jet-flow temperature was controlled by means of a heat exchanger and electrical blankets, in order to avoid possible condensation of NO_2 in the pipe-line and to equalize the temperatures of both jet-flow and the crossflow during the course of the experiments. So, possible variations in the tracer-concentration due to variation in the equilibrium between NO_2 and N_2O_4 (up to 25%) [14] and variations in the density of the flows and consequently in the adjusted momentum ratio (up to 3%) could be minimized. The measurements were carried out employing a measuring section with extended optical access, which is described in [12].

The used measuring technique, introduced in detail in [9], consists of two classical laser diagnostic methods: particle image velocimetry PIV and laser induced fluorescence LIF. Both systems were used simultaneously, and thus, allowing spatial measurements of the instantaneous velocity and concentration fields at the same time. A schematic illustration of this 2d-LIF-PIV system is given in Fig. 2. One laser light sheet from a frequency doubled, double pulse Nd:YAG-laser was used to generate the PIV- and the LIF-signal. The induced PIV-signal, light scattered from the droplets at 532 nm as well as the LIF signals of the broadband stokes-shifted fluorescence from the molecular tracer NO_2 (between 540 – 700 nm) are imaged perpendicularly to the the laser sheet by two appropriate cameras, a CCD-camera (1024 $\times$ 1024 pixels) for the PIV-System and an ICCD-camera (512 $\times$ 512 pixels) for the LIF-system. The signals were separated by means of a dichroic mirror. After acquisition of the data, the signals were analyzed using the software Dantec/FlowManager Version 4.71 and a Matlab routine. Every generated image was 24 $\times$ 24 mm in size. In each image, velocity vectors were calculated using interrogation areas of 32 $\times$ 32 pixels in size.

In Fig. 2 the employed coordinate convention is also represented. The origin of the coordinate system is located in the center of jet outlet. The x- and y-directions correspond to the axial (streamwise) and the lateral (spanwise) directions of the crossflow respectively, the z-direction to the axial direction of the jet flow.

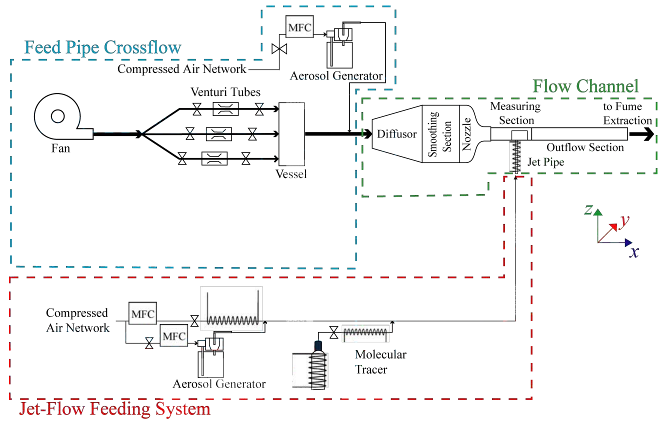

FIGURE 1. SCHEMATIC ILLUSTRATION OF THE JET-IN-CROSSFLOW-ARRANGEMENT.

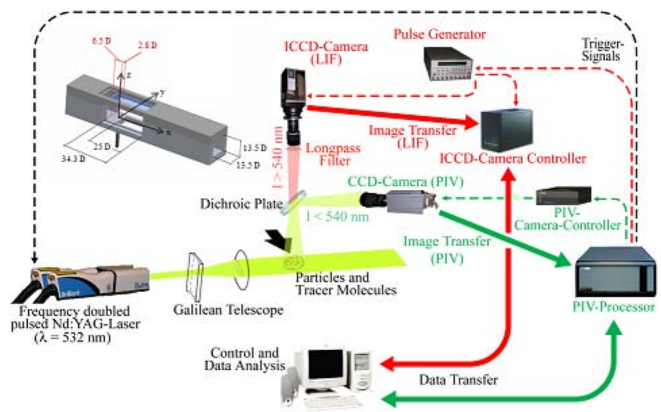

FIGURE 2. EXPERIMENTAL SET-UP OF THE SIMULTANEOUS 2d-LIF-PIV MEASURING TECHNIQUE. ADDITIONALLY, THE MEASURING SECTION AND THE LOCATION OF THE COORDINATE SYSTEM ARE GIVEN.

Flow Conditions

The experiments were performed for two different JCF-cases, which will be referred to as Case *I* and Case *II*. They have the same jet flow-rate and are characterized by the values listed in Table 1.

Case *I* presents also the property that its flow conditions have been already investigated [12, 13] and therefore it can be considered as a reference case, making possible a crosscheck of the experimental results obtained here with previous works.

With the aim to characterize the inflow conditions of the crossflow, different velocity profiles of the crossflow (without the jet-flow) were determined in the middle plane of the measuring section (y = 0) using PIV. Figure 3 shows selected time averaged velocity profiles of the crossflow (without jet-flow) in the *x*-

TABLE 1. EXPERIMENTAL PARAMETERS FOR THE SIMULTANEOUS 2d-LIF-PIV-MEASUREMENTS.

	case:	I	II
Crossflow	Re_∞	$60{\cdot}10^3$	$40{\cdot}10^3$
	U_∞ [m/s]	9.08	6.04
	D_∞ [m]	0.108	0.108
Jet-Flow	Re_j	$18{\cdot}10^3$	$18{\cdot}10^3$
	U_j [m/s]	37.72	37.72
	D [m]	0.008	0.008
$R = U_j/U_\infty$		4.15	6.25

and the z-directions $< u_\infty >$, $< w_\infty >$ for both investigated cases. Dashed lines represent the Case I and dash-dot lines Case II. It can be recognized on Fig. 3 that the crossflow inflow conditions in the measuring section for both cases correspond, as expected, to a "plug-flow" velocity profile. Such a flow characteristic can be attributed to the usage of an appropriate contraction nozzle at the inlet of the measuring section, such as explained in [9]. It is also observed in Fig. 3 that the measured component of the mean crossflow velocity in the z-direction $< w_\infty >$ tends to zero in both cases, which indicates the uniformity of the flow in the measuring section. The discontinuity seen around $z/D = 2$ are caused by the reflections of the laser-light from the bottom of the channel, which affect the obtained PIV-signal and hence the signal-to-noise-ratio, therefore it can be assumed that the upper boundary layer (at z/D = 108 mm / 8 mm = 13.5) for each case is similar to the corresponding boundary layer at the bottom of the channel. The turbulence intensity of the crossflow in the x-direction $Tu_x = \sigma(u)/ < u > \times 100\%$ was determined to be smaller than 2% in the core of the crossflow (not shown in the figure).

Jet-flow velocity profiles were obtained without crossflow at a height of 4 mm ($z/D = 0.5$) and higher above the jet exit in its middle plane ($y = 0$). A selected profile of the jet velocity in the z-direction $< w_j >$ is shown in Fig. 4 together with its corresponding standard deviation σ_w. It can be recognized there, that the jet-flow has a turbulent fully developed profile, where the maximal value of the velocity component in the z-direction approximates to $5/4{\cdot}U_j$, which is the quantity reported in the literature for such a case [15]. It is also observed, that the standard deviation of the velocity in the z-direction has its minimum value around the flow-axis and its maximum close to the pipe-wall. The latter is due to the influence of the boundary layer on the jet-flow in the pipe. In the core of the jet-flow, a turbulence intensity in the z-direction $Tu_z = \sigma_w / < w_j > \cdot 100\%$ less than 6% can be estimated.

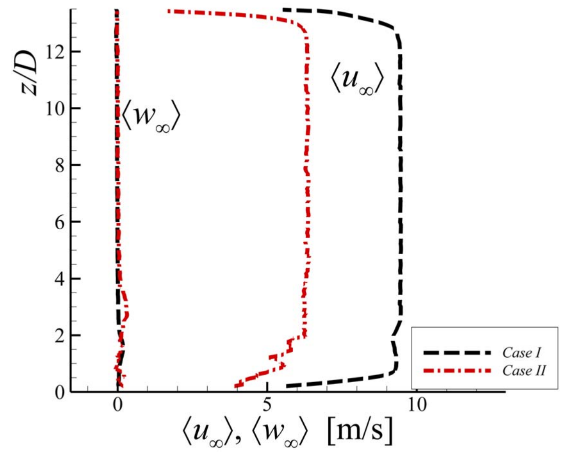

FIGURE 3. TIME AVERAGED VELOCITY-COMPONENTS OF THE CROSSFLOW IN THE x- AND THE z-DIRECTIONS $\langle u_\infty \rangle$, $\langle w_\infty \rangle$ IN [m/s]. DATA OBTAINED 16 mm UPSTREAM (x/D = -2) OF THE JET-OUTLET CENTER ALONG $0 < z/D < 13.5$ IN THE MIDDLE VERTICAL PLANE $y = 0$.

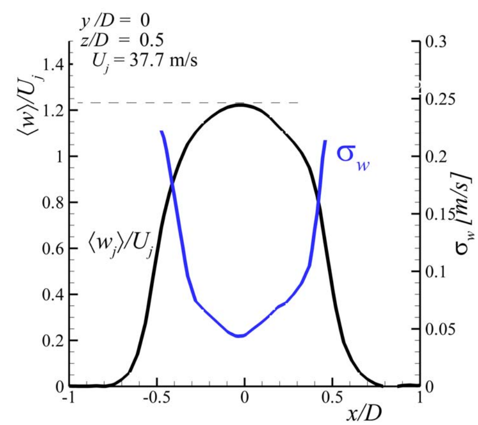

FIGURE 4. DIMENSIONLESS AVERAGED VELOCITY COMPONENT IN THE z-DIRECTION $\langle w \rangle / U_j$ OF THE JET-FLOW (WITHOUT CROSSFLOW) AND ITS CORRESPONDING STANDARD DEVIATION σ_w. U_J REPRESENTS THE JET-FLOW BULK VELOCITY (= 37.7 m/s). DATA GAINED ON THE CENTER PLANE $y = 0$ AT A HEIGHT $z/D = 0.5$

RESULTS AND DISCUSSION

In the present section results of the diverse experiments performed are presented. The spatial coordinates x, y and z have been normalized by the jet diameter D = 8mm, and the velocities u, v and w in the x-, y- and z-directions respectively by the bulk

TABLE 2. ESTIMATED UNCERTAINTY OF THE EXPERIMENTAL RESULTS.

Variable	Uncertainty [%]
w	± 1
u	± 7
c	± 5
w'	± 1
u'	± 9
c'	± 7
$u'u'$	± 2
$w'w'$	± 13
$u'w'$	± 12
$u'c'$	± 12
$w'c'$	± 7

velocity of the crossflow U_∞ (if not otherwise specified). For Case *I*: U_∞ = 9,08 m/s and for Case *II*: U_∞ = 6,04 m/s. For both investigated cases, measurements were carried out in the symmetry plane $y = 0$ and at different horizontal planes, z/D = 1.0; 1.5; 2.0; 2.5 and 4.5 for Case *I* and z/D = 1.0, 2.5 and 4.5 for Case *II* [16]. Due to the fact that the symmetry plane provides more representative general information of a JCF than the horizontal ones, the majority of the results presented in this work are referred to this plane.

In general, each measured plane consisted of 9 frames (9 camera-positions) and each frame results from the average of 2400 pictures or rather picture-pairs (for the PIV-System). These images were collected at a rate of 2.7 Hz which is sufficiently slow to assume independence of the data in time, allowing efficient sampling to achieve statistically converged results with minimal data. Uncertainty analysis of the velocity and concentration statistics was carried out using the root-sum-square (RSS) technique described by Moffat [17] and the resulting uncertainty for all variables are summarized in the Table 2.

Jet trajectory

One of the most important characteristics of a JCF is the so-called penetration of the jet into the crossflow. This penetration is normally evaluated by means of the jet trajectory. There are different ways to determine the jet trajectory in a JCF, such as the streamline trajectory, the maximal velocity trajectory or the maximal concentration trajectory, among others [1, 8, 18, 19]. In the literature, the trajectory which is defined as the mean streamline

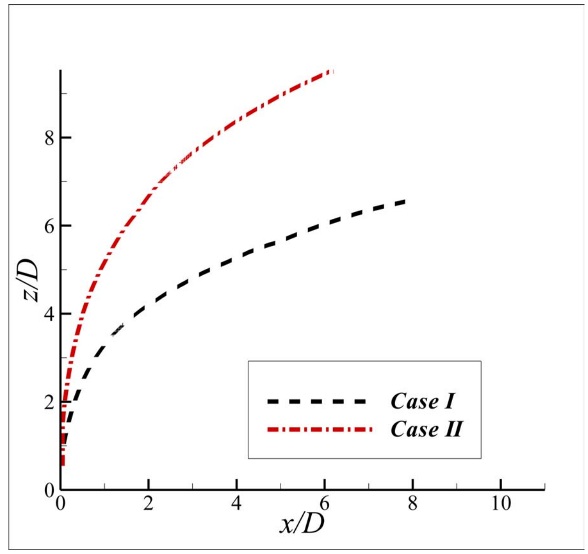

FIGURE 5. STREAMLINE JET TRAJECTORIES FOR CASE *I* (DASHED LINE) AND CASE *II* (DASH-DOT LINE).

originates in the middle of the jet at its outlet "streamline trajectory" is often used as a reference. Figure 5 shows the streamline trajectories for both investigated cases. The represented streamlines begin at a z/D value of 0.5, the deepest z/D-coordinate of the measurement vertical planes, to be able to warrant a good signal to noise ratio. At this figure it is evident that the expected trend has been reproduced. The penetration of the jet into the crossflow increases with increasing of the velocity ratio.

Pratte and Baines (1967) [20] proposed from a dimensional analysis the following general form for the streamline trajectory:

$$\frac{z}{D \cdot r} = A \cdot \left(\frac{x}{D \cdot r}\right)^b . \tag{1}$$

where A and b are experimental constants, which can be found in the literature in the range of $1.2 < A < 2.6$ and $0.28 < b < 0.34$. Often cited values for the parameters are reported in [20]: A = 2.05 and b = 0.28. In this regard, an extensive list of experimental values for these parameters A and b have been collected in Margason (1993) [4]. In Fig. 6 are plotted on log-log scales the streamline trajectories from both studied cases using Dr-normalized coordinates. It is recognized that from a coordinate $x/D = 0.2r$ both trajectories have the same constant gradient. This range is defined in the literature as the "power-law" region [1] and for the two cases presented here the exponent of the power law was b = 0.33. The leading coefficient A for Case *I* was 1.3 and for Case *II* 1.55. The obtained values of A and b agree well with the mentioned range found in the literature. On the other hand, the difference of the values of A in both cases

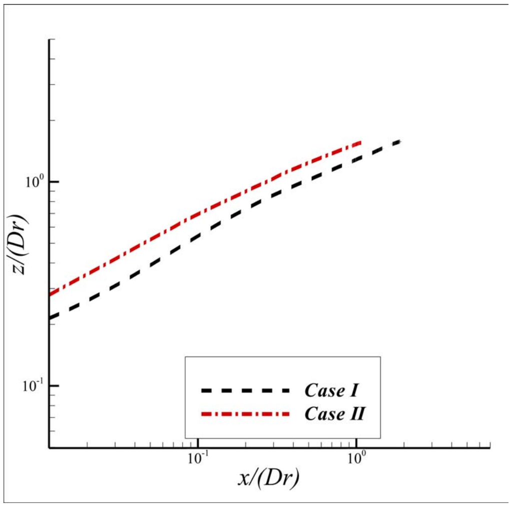

FIGURE 6. STREAMLINE JET TRAJECTORIES FOR CASE *I* (DASHED LINE) AND CASE *II* (DASH-DOT LINE) IN *Dr*-NORMALIZED COORDINATES.

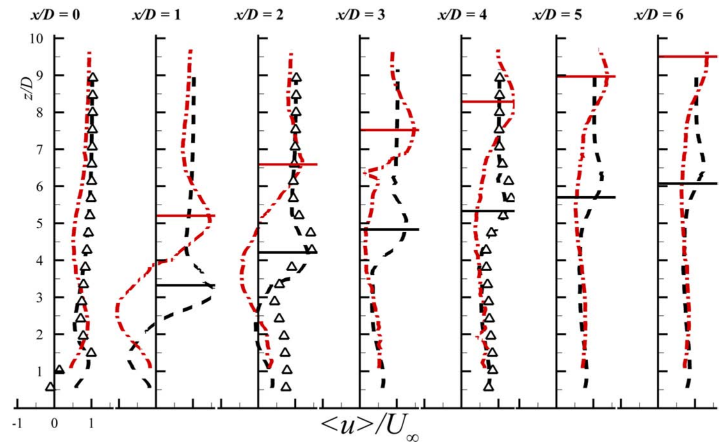

FIGURE 7. VERTICAL PROFILES OF THE AVERAGED VELOCITY COMPONENT IN x-DIRECTION AT $y/D = 0$ (LINES) AND $y/D = 0.5$ (TRIANGLES) BY DIFFERENT x/D-COORDINATES. CASE I: DASHED LINES ($y/D = 0$) AND TRIANGLES ($y/D = 0.5$), CASE II: DASH-DOT LINES.

can be attributed to the difference of the crossflow velocity and hence of the velocity ratio r. The boundary layer thickness of the crossflow may also have an influence in the jet-trajectory, as reported in the literature [21].

Figure 7 and Fig. 8 show exemplary line-plots of the averaged velocity component in the x-direction and of the averaged concentration on the center plane $y = 0$ at different x-positions for both cases. Dashed lines represent the measurements of Case *I* and dash-dot lines correspond to Case *II*. Additionally, the positions of the corresponding streamline trajectories for each x/D-coordinate are also shown as solid horizontal lines – dark line for Case *I* and light line for Case *II*. At these figures it can be seen again, that the penetration of Case *I*, with smaller velocity ratio, is smaller than the penetration of Case *II*. Furthermore, it can be recognized in both investigated cases that the z/D-coordinate of the maximal concentration (or the lowest coordinate of maximal concentration, when the scalar profiles have multiple local maxima) is smaller than the corresponding z/D-coordinate of the streamline trajectory at the same x/D-coordinate, whereas the z/D-coordinate of the maximal velocity coincides practically with the streamline trajectory in the region close to the jet outlet ($x/D < 3$) and then rises more quickly than the streamline trajectories (more evident in Case *I*). This behavior corresponds to the trend of the local maximal concentration and velocity trajectories reported in the literature [1, 19, 22]. Additionally, it can be observed, that in Case *I* there is a greater difference between the streamline and the maximal concentration z/D-coordinates and hence trajectories than in Case *II*, which is consistent with the finding by Kamotani and Greber (1972) [22], that the lower the trajectory, the greater the difference between streamline and maximal concentration trajectories.

Figure 7 shows also data of the averaged velocity component in x-direction for Case I at $y/D = 0.5$ for only $x/D = 0$; 2 and 4 (triangles). It is appreciated, that in the near-field region ($x/D < 3$) these profiles differs from the ones obtained at the center plane $y = 0$, but the profiles from both vertical planes at $x/D = 4$ are quite similar. It is due to the jet flow in the far-field region has been spread and consequently the jet core has been transformed to a kidney-like shape causing that the profiles in this region trend to be similar. The vertical velocity profiles at Fig. 7 for Case *I* at $y = 0$ agree very well with the data reported by Galeazzo et. al [12] (not shown in the figure).

On the other hand, Fig. 8 shows also for $x/D = 1$ and 6 vertical concentration profiles gained using a testing probe for Case *I* (circles). For this test CO_2 was fed in the jet-flow (5%) instead of NO_2, and an infrared analyzer (BINOS / Leybold-Heraeus, 0-5%) was employed to determine the corresponding concentration in the measuring section. A very good agreement between both measuring techniques (testing probe - LIF) was found.

Scalar concentration-maps

Figure 9 shows the normalized mean jet concentration maps $< c >$ for two different z/D-heights of both investigated cases. $< c >$ is given by the ratio $< C_{NO_2} > / C_{NO_2,j}$, in which $< C_{NO_2} >$ represents the local concentration of NO_2 and $C_{NO_2,j}$ the NO_2-concentration in the jet. The mean flow is symmetric at the plane $y/D = 0$, therefore only the half range is represented here. The upper part of each 2d-plot represents the Case *I*, whereas the case.

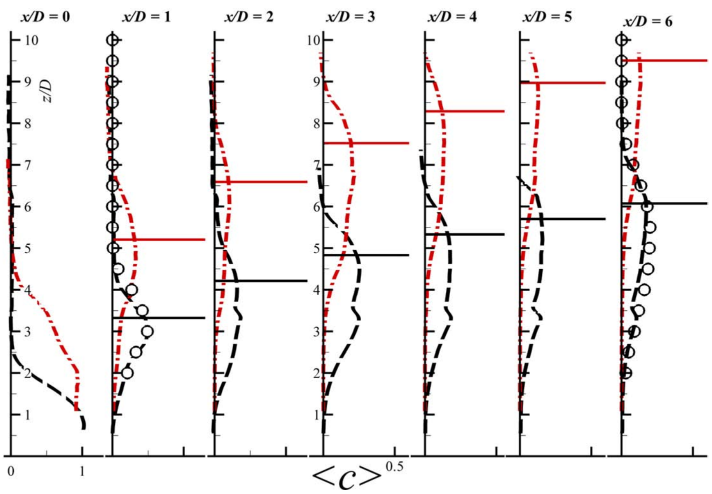

FIGURE 8. VERTICAL PROFILES OF THE AVERAGED NORMALIZED JET-CONCENTRATION ON THE CENTER PLANE y/D = 0 BY DIFFERENT x/D-COORDINATES FOR CASE I (DASHED LINE) AND CASE II (DASH-DOT LINE). CIRCLES REPRESENT CONVENTIONAL CONCENTRATION MEASUREMENTS WITH A TESTING PROBE FOR CASE I.

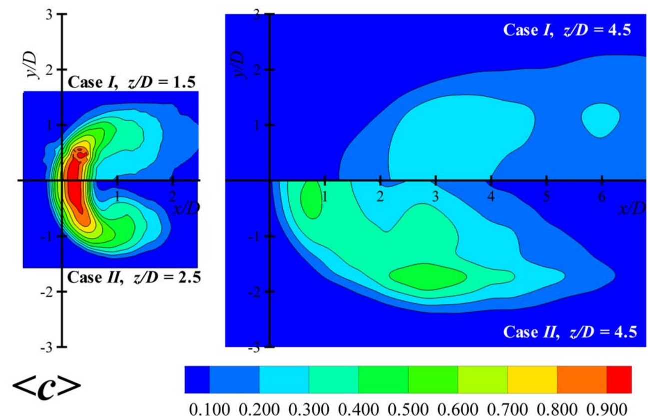

FIGURE 9. NORMALIZED MEAN JET CONCENTRATION MAPS FOR DIFFERENT z/D-HEIGHTS. CASE I IS REPRESENTED AT THE SUPERIOR SECTOR EACH MAP AND CASE II AT THE INFERIOR SECTOR.

Case II is represented in the lower part of the same plot. On the left side results at lower measurement positions are shown. Here, results at z/D = 1.5 for Case I are compared with z/D = 2.5 for Case II. These planes were selected, since they represent similar jet curvatures (cf. Fig. 5). This similarity can be also verified by means of the coincidence of the maximal concentration position in both cases. This structure indicates that for both cases the jet core remains relatively unmixed, however a higher level of dispersion of the jet-concentration is found in Case I, what reveals a better mixing. This phenomenon can be attributed to the fact that the crossflow turbulence level for Case I is higher than for Case II, which increases the intensity of the interaction between the jet- and the crossflow, although the jet-flow in Case II has further propagated into the crossflow. Due to the jet-flow having bent by the crossflow momentum by only a small amount at these heights, it is also possible to recognized there the kidney-shape structure characteristic of the most important mean-flow feature of a JCF, the counter-rotating vortex pair [3].

The right side of Fig. 9 shows a comparison of normalized mean concentration maps at z/D = 4.5 for both cases. As expected, in Case I (upper part of the figure) the jet concentration is found further downstream than in Case II, because the jet-flow has been already bent by the crossflow. Additionally, the flow configuration in Case I appears to be better mixed than in Case II at this height, which can also be attributed to the fact that in Case I there is a more intensive interaction between both flows due to the already mentioned higher crossflow momentum in this case.

Reynolds-fluxes and -stresses

In Fig. 10 2d-plots of the normalized Reynolds-fluxes $< u'c' > /U_\infty$ in the x-direction (at the left) and Reynolds-stresses $< u'w' > /(U_\infty U_j)$ (at the right) are given for both Case I (top) and Case II (bottom) at the symmetry plane. The velocity component in the x-direction u was normalized with the crossflow bulk velocity U_∞, whereas the one in the z-direction w with the jet bulk velocity U_j. It becomes obvious that the represented Reynolds fluxes and Reynolds stresses structures are quite similar in form and in magnitude for the same case, which is an indication that the turbulent transport of momentum and mass is similar. In the considered region the jet flow is mainly characterized by the normalized jet-concentration $< c >$ and the velocity component in the z-direction $< w > /U_j$. Consequently, the physical quantities depicted in the maps of Fig. 10 reflect the enhanced fluxes of a turbulent flow compared to a laminar one caused by the fluctuations of the turbulent flow, hence they are very important in the implementation of a benchmark. Thus, the fluctuations of the jet concentration depict the turbulent mass transport as well as the fluctuations of the velocity component in the z-direction the momentum exchange. Focused in the quantities represented in Fig. 10, the considered transport and exchange is carried out in the x-direction. It is also recognized in this figure, that the intensity of the correlation between u' and c' is slightly higher than the correlation between u' and w'. It can be explained by the fact that for the considered medium (air) the Schmidt number, defined as the ratio between momentum diffusivity (viscosity) and mass diffusivity, is slightly smaller than 1.0; consequently the mass transport is slightly more intense than the momentum exchange. On the other hand, a change of the correlation sign is also observed. This change is due to the fact that the velocity component in the x-direction u in the region directly downstream of the jet outlet presents a change of the direction sense and consequently of sign (cf. Fig. 7), therefore the correlations $< u'c' > /U_\infty$ and $< u'w' > /(U_\infty U_j)$ downstream as well as upstream of the jet outlet are similar.

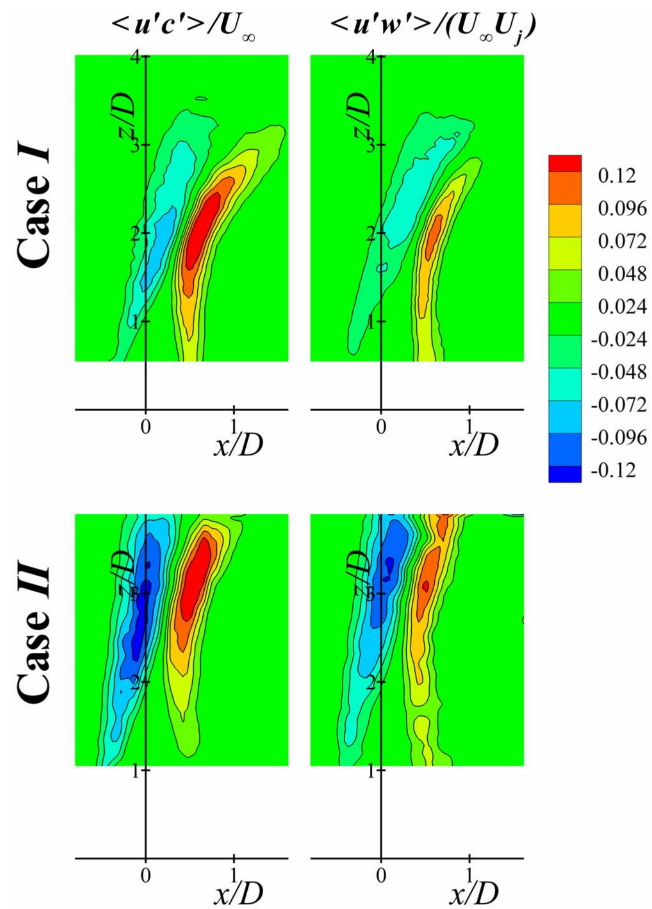

FIGURE 10. NORMALIZED REYNOLDS-FLUXES $< u'c' > /U_\infty$ (LEFT) AND -STRESSES $< u'w' > /(U_\infty U_j)$ (RIGHT) FOR CASE *I* (TOP) AND *II* (BOTTOM) AT THE SYMMETRY PLANE $y = 0$.

Analogue to Fig. 10, 2d-plots of the normalized Reynolds-fluxes $< w'c' > /U_j$ in the z-direction (at the left) and Reynolds-stresses $< w'w' > /(U_j U_j)$ (at the right) are given in Fig. 11. Likewise to Fig. 10, it is found that the shape of these quantities in the represented range are quite similar. Nevertheless, it is observed that the intensity of the Reynolds-stresses are larger

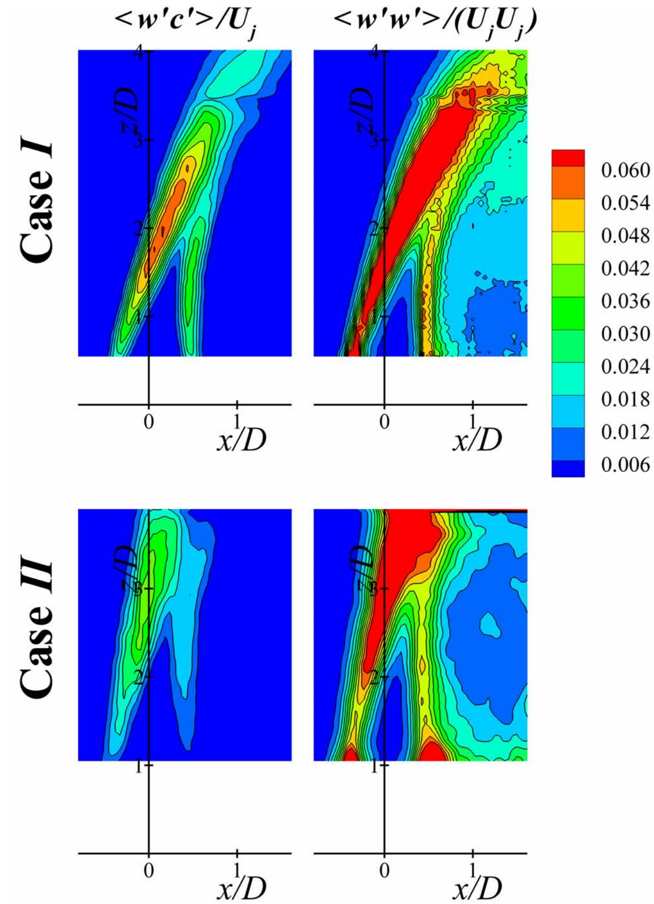

FIGURE 11. NORMALIZED REYNOLDS-FLUXES $< w'c' > /U_j$ (LEFT) AND -STRESSES $< w'w' > /(U_j U_j)$ (RIGHT) FOR CASE *I* (TOP) AND *II* (BOTTOM) AT THE SYMMETRY PLANE $y = 0$.

than the one of the Reynolds-fluxes in the z-direction; mainly from x/D-coordinates larger than 1, as can be also observed in the Fig. 12b, at which a quantitative comparison of these quantities is shown. This elevated intensities of the Reynolds-stresses can be attributed to the entrainment of the crossflow into the jet-flow in the z-direction, which is not detected by means of the Reynolds-fluxes, because only the jet-concentration is detected and therefore a correlation between the jet-flow and the whole movement in the z-direction is not possible.

As mentioned above, Fig. 12a and b show line comparisons of the quantities presented in Fig. 10 and 11 as well.

CONCLUSION

Using the non intrusive 2d-LIF and PIV measurement techniques at a jet in crossflow arrangement, experimental two-dimensional maps of concentrations (2d-LIF) and velocities (PIV) were gained simultaneously for two different cases under

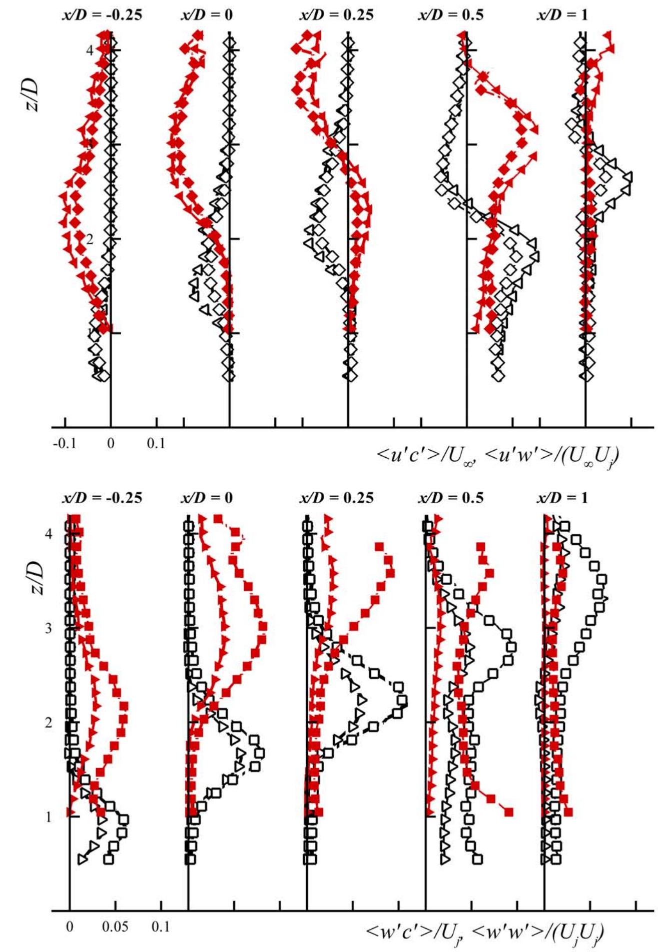

FIGURE 12. VERTICAL PROFILES OF THE NORMALIZED REYNOLDS-FLUXES(TRIANGLES) AND -STRESSES (RECTANGLES) IN THE x-DIRECTION (UPPER FIGURES) AND IN THE z-DIRECTION (LOWER FIGURES) ON THE CENTER PLANE $y = 0$ BY DIFFERENT x/D-COORDINATES. CASE *I*: BLACK LINES, CASE *II*: RED LINES.

highly turbulent conditions. For PIV-measurements, droplets of DEHS (Di-Ethyl-Hexyl-Sebacat) were added to both air flows, the jet- and the crossflow, and NO_2 was added only to the jet flow as molecular tracer for the LIF-system. The NO_2 was chosen because it absorbs the light at the wavelength of the frequency-doubled Nd:YAG-laser used for the PIV-measurements. From this simple combination of only one laser and two appropriate CCD-cameras, it was possible to acquire not only instantaneous values of velocity and concentration but also the full statistical information of the measured quantities. Consequently, mean values, standard deviations, turbulence intensities, variances, Reynolds-fluxes and -stresses could be obtained in 2d-maps.

A comparison between the two studied cases with different velocity ratios r was performed, which confirmed that the penetration of the jet into the crossflow rises with increasing velocity ratio. The streamline trajectories of the studied cases were fit according to the jet trajectory equation (eqn.1) and the obtained parameter matched the range reported in the literature.

In the near-field of the jet outlet the jet is mainly characterized by the jet-concentration and the velocity component in the z-direction. Therefore, the jet bulk velocity was used to normalize velocities in the z-directions. As a consequence, it was observed that the Reynolds-fluxes $< u'c' > /U_\infty$ in the x-direction and the Reynolds-stress-component $< u'w' > /(U_\infty U_j)$ are quite similar in regard to magnitude and size of the spatial distribution, which is an indication that the transport of momentum and mass are similar.

ACKNOWLEDGMENT

The authors gratefully acknowledge the Ministry of Research of Baden-Württemberg, Germany, together with Siemens AG Germany within the special research initiative *"Kraftwerke des 21. Jahrhunderts"* ("Power Plants of the 21th Century") for its financial support. The authors would also like to thank Prof. Dr. habil. R. Suntz for his valuable contribution to the measurement technique and Dr.-Ing. P. Habisreuther for the fruitful and stimulating discussion.

REFERENCES

[1] Yuan, L.L., and Street, R.L., 1998. "Trajectory and entrainment of a round jet in crossflow". *Physics of Fluids,* ***10***(9), pp. 2323–2335.

[2] Muppidi, S., and Mahesh, K., 2008. "Direct numerical simulation of passive scalar transport in transverse jets". *J. Fluid Mech.,* ***598***, pp. 335–360.

[3] Broadwell, J., and Breidenthal, R., 1984. "Structure and mixing of a transverse jet in incompressible flow". *J. Fluid Mech.,* ***148***(405).

[4] Margason, R., 1993. "Fifty years of jet in cross flow research". In Computational and Experimental Assessment of Jets in Cross Flow, CP-534, AGARD.

[5] Hasselbrink, E., Mungal, M., and Hanson, R., 1997. "Planar velocity measurements and OH imaging in a transverse jet flame". In Proceeding, ASME, ed., Vol. **1** of *35th Aerospace Sciences Meeting and Exhibit*, pp. 118 – 130.

[6] Carter, C., Donbar, J., and Driscoll, J., 1998. ""Simultaneous CH planar laser-induced fluorescence and particle imaging velocimetry in turbulent non-premixed flames"". *Applied Physics B: Lasers and Optics,* ***66***, pp. 129–132.

[7] Su, L., and Mungal, M., 1999. "Simultaneous measurements of velocity and scalar fields: application in cross-

flowing jets and lifted jet diffusion flames". In *Center of Turbulence Research, Annual Research Briefs*. -, pp. 19–35.

[8] Hasselbrink, E., and Mungal, M., 2001. "Transverse jets and jet flames. Part 2. Velocity and OH field imaging". *Journal of Fluid Mechanics,* ***443***, pp. 27–68.

[9] Cárdenas, C., Suntz, R., Denev, J. A., and Bockhorn, H., 2007. "Two-dimensional estimation of Reynolds-fluxes and -stresses in a Jet-in-Crossflow arrangement by simultaneous 2D-LIF and PIV". *Applied Physics B: Lasers and Optics,* ***4***, pp. 581–591.

[10] Oezcan, O., Meyer, K., and Westergaard, C., 2001. "Simultaneous measurements of velocity and concentration in a jet in channel-crossflow". In *Proceeding*, ASME, ed., Vol. of *FEDSM, ASME Fluids Eng. Div. Summer Meeting, New Orleans, USA*. ASME, May, pp. 1–12. Paper number 18220.

[11] H. Bockhorn, D. Mewes, W. P. H. W., ed. *Micro and Macro Mixing – Analysis Simulation and numerical Calculation*, 1^{st} ed., Vol. 1 of *Springer series on Heat and Mass Transfer*. Cárdenas, C. and Suntz, R. and Bockhorn, H., Experimental Investigation of the Mixing-Process in a Jet-in-Crossflow Arrangement by Simultaneous 2d-LIF and PIV, Chap. 2, pp. 87–103.

[12] F.C.C.Galeazzo, G.Donert, P.Habisreuther, N.Zarzalis, R.J.Valdes, and W.Krebs, 2010. "Measurement and Simulation of Turbulent Mixing in a Jet in Crossflow". In Proceeding, ASME, ed., Vol. **1** of *ASME Turbo Expo 2010: Power for Land, Sea and Air (CDROM)*, ASME, ASME, pp. 1–12. Paper number GT2010-22709.

[13] Galeazzo, F.C.C., Donert G., Habisreuther, P., Zarzalis, N., Valdes, R.J., and Krebs, W., 2011. "Measurement and Simulation of Turbulent Mixing in a Jet in Crossflow.". *Journal of Engineering for Gas Turbines and Power*, p. in press.

[14] Roscoe, H.K., and Hind, A.K., 1993. "The Equilibrium Constant of NO_2 with N_2O_4 and the Temperature Dependence of the Visible Spectrum of NO_2: A Critical Review and the Implications for Measurements of NO_2 in the Polar Stratosphere.". *Journal of Atmospheric Chemistry,* ***16***, pp. 257–276.

[15] Bird, Robert Byron ; Stewart, W. E. . L. E. N., 2002. *Transport phenomena*, 2. ed. ed. Wiley, New York.

[16] Sedlmaier, J., 2010. "Experimentelle Untersuchung des Einflusses der Reynolds-Zahl auf die Vermischung in einer Jet-in-Crossflow Anordnung". Thesis, Karlsruhe Institute of Technology, Karlsruhe, Germany, Sep.

[17] Moffat, R.J., 1988. "Describing the uncertainties in Experimental Results.". *Experimental Thermal and fluid Science,* ***1***, pp. 3 – 17.

[18] Hasselbrink, E., and Mungal, M., 2001. "Transverse jets and jet flames. Part 1. Scaling laws for strong transverse jets". *Journal of Fluid Mechanics,* ***443***, pp. 1–25.

[19] Denev, J., Froehlich, J., and Bockhorn, H., 2007. "Direct numerical simulation of a transitional jet in crossflow with mixing and chemical reactions.". In Proceeding, J. E. J. H. N. K. M. L. R. Friedrich, N.A. Adams, ed., Vol. **1** of *5th Int. Symp. on Turbulence and Shear Flow Phenomena, TU-Munich, Garching, Germany*, pp. 1243 – 1248.

[20] Pratte, B., and Baines, W., 1967. "Profiles of the round turbulent jet in a cross flow". *J. Hydraul. Div ASCE,* ***6***, pp. 53–63.

[21] Muppidi, S., and Mahesh, K., 2005. "Study of trajectories of jets in crossflow using direct numerical simulations". *J. Fluid Mech.,* ***520***, pp. 81–100.

[22] Kamotani, Y., and Greber, I., 1972. "Experiments on a turbulent jet in a cross flow". *AIAA J.,* ***10***, pp. 1425–1429.